Front. Chem. Sci. Eng. 2020, 14(1): 105–111
https://doi.org/10.1007/s11705-019-1791-6

COMMUNICATION

Highly selective detection of copper(II) by a “ligand-free” conjugated copolymer in nucleophilic solvents

Weixing Deng[1], Pengfei Sun[1], Quli Fan (✉)[1], Lei Zhang[1], Tsuyoshi Minami (✉)[2]

1 Key Laboratory for Organic Electronics and Information Displays & Jiangsu Key Laboratory for Biosensors, Institute of Advanced Materials (IAM), Jiangsu National Synergetic Innovation Center for Advanced Materials (SICAM), Nanjing University of Posts & Telecommunications, Nanjing 210023, China
2 Institute of Industrial Science, The University of Tokyo, Meguro-ku, Tokyo 153-8505, Japan

Abstract The synthesis of *N*-cyclohexyl carbamate-attached fluorene-*alt*-phenylene copolymer (PFPNCC) and the use of PFPNCC as a “ligand-free” fluorescent chemosensor for Cu(II) are described. Addition of Cu(II) can efficiently quench the fluorescence of PFPNCC in nucleophilic solvents such as DMF and DMSO, but not in low nucleophilic solvents such as 1,4-dioxane and THF. Ultraviolet-visible spectra of the mixture of the conjugated polymer and Cu(II) indicate the presence of a reduced Cu (I) ion in the solution. Furthermore, fluorescence recovery of PFPNCC observed at low temperature suggests that the quenching and reducing mechanism is most probably due to a photo-induced electron transfer from excited PFPNCC to Cu(II). Our findings provide a novel strategy for highly selective conjugated polymer-based chemosensors for various target analytes, albeit “ligand-free”.

Keywords ligand-free, fluorescent chemosensor, copper, photo-induced electron transfer

1 Introduction

Copper ions, the third abundant trace metal ions in human body, are often employed for metal centers of over 30 proteins [1,2] such as superoxide dismutase, ceruloplasmin, lysyl oxidase, cytochrome c oxidase, tyrosinase and dopamine-β-hydroxylase [3–5]. Although copper ions play a positive role in human body, their disorder induces various neurodegenerative diseases [6–9]. In addition, the contamination of environmental water by copper ions leads to heavy-metal pollution, because certain microorganisms are affected by even sub-μmol/L concentrations of copper ions [10]. In this regard, World Health Organization (WHO) recommends that the concentration of copper ions in drinking water must not exceed 2 mg/L (30 μmol/L) [11]. Therefore, much attention has been paid to the selective recognition and sensing of copper ions.

Fluorescent chemosensors for copper ions have attracted considerable interest, because the conventional methods, including high performance liquid chromatography, mass spectrometry and atomic absorption spectroscopy, suffer either from expensive procedures or the use of sophisticated instruments [12]. To date, a variety of fluorescent chemosensors with copper ion ligands such as pyridine [13,14], Schiff-base [15], crown ether [16], and their derivatives has been developed. Moreover, conjugated polymers have emerged as one of the most important classes of backbone and reporter moieties for chemosensors [17]. A key advantage of conjugated polymer-based chemosensors is their potential to exhibit collective properties that are sensitive to very minor perturbations [18]. Thus, several conjugated polymer-based chemosensors with bipyridine or imidazole have been developed for the detection of copper ions [19–21]. Most of the reported chemosensors have copper chelating sites linked to reporter-backbones [22–24]. However, these chemosensors suffer from complicated synthesis and interference from competing metal ions. Hence, the development of a highly selective and simple detection strategy for copper ions “without” any ligand cites remains a challenge.

We herein report a “ligand-free”, *N*-cyclohexyl carbamate-attached fluorene-*alt*-phenylene copolymer (PFPNCC) as a highly selective fluorescent chemosensor for copper ions. The bulky side-chain, *N*-cyclohexyl carbamate, can improve the solubility of the π-conjugated polymer. More importantly, the fluorescence of PFPNCC can be quenched by Cu(II) in nucleophilic solvents. To the best of our knowledge, this is the first time to report a

Received August 22, 2018; accepted October 27, 2018

E-mails: iamqlfan@njupt.edu.cn (Fan Q);
tminami@iis.u-tokyo.ac.jp (Minami T)

conjugated copolymer-based chemosensor for Cu(II) without any metal ligands in molecular structures.

2 Experimental

2.1 Materials

All chemical reagents and organic solvents used were purchased from Sigma-Aldrich, Acros, and Alfa and were used without further purification. All organic reactions were performed under a nitrogen atmosphere.

2.2 Methods

NMR spectra were recorded on a Bruker Ultra Shield Plus 400 MHz. Gel permeation chromatography analysis of PFPNCC was conducted on Shim-pack GPC-80X columns with THF as an eluent and polystyrenes as standard polymers. Ultraviolet-visible spectroscopy (UV–vis) and fluorescence spectroscopic measurements were performed on a Shimadzu UV–3600 and a Shimadzu RF-5301PC spectrophotometer, respectively. The solutions of metal ions were prepared by dissolving an appropriate amount of metal salts in Milli-Q grade water. To evaluate the metal ion detectability of PFPNCC, the aqueous solutions with metal ions were added into a *N*,*N*-dimethylformamide (DMF) solution (2 mL) of PFPNCC (1.0×10^{-6} mol/L).

2.3 Synthesis of PFPOH

Monomer units were synthesized according to the previously reported methods [25,26]. 0.744 g (1.00 mmol) of (9,9-bis(6-bromohexyl))fluorene-2,7-diboronic acid di(pinacol) ester (**1**), 0.384 g (1.00 mmol) of 1,4-dibromo-2,5-di(hydroxypropyloxy)-benzene (**2**) and 1 mol-% of $Pd(PPh_3)_4$ were placed into a two-neck flask. Subsequently, 30 mL of 1,4-dioxane and 2 mL of an aqueous solution with 0.69 g (5.00 mmol) of K_2CO_3 were added to the flask. The resulting mixture was stirred at 85°C for 3 d. After this period, phenylboronic acid (5 mol-%) was added, and the mixture was further heated at 85°C for 8 h. Then, bromobenzene (5 mol-%) was added to the mixture and stirred at 85°C for 16 h. After cooling down, 1,4-dioxane was removed in vacuo and the residue was dissolved in dichloromethane. The dissolved residue was purified by an alumina column chromatography. The collected solution was partially concentrated, followed by reprecipitation by using in *n*-hexane. In this way, 0.7 g of PFPOH was obtained. Yield: 56%. ^1H NMR (400 MHz, $CDCl_3$, δ ppm): 7.28–7.86 (m, 6H, fluorene–H), 7.20 (s, 2H, phenylene–H), 4.15 (t, J = 5.6 Hz, 4H, Ar–O–CH_2–), 3.77–4.10 (m, 8H, –CH_2OH, –CH_2Br), 2.07 (quint., J = 8.8 Hz, 4H, –CH_2–CH_2OH), 1.80–1.90 (m, 8H, –CH_2–CH_2Br, fluorene–CH_2–), 1.17–1.40 (m, 12H, –CH_2–).

2.4 Synthesis of PFPNCC

PFPOH (0.2 g) was dissolved in 20 mL of dry 1,4-dioxane at room temperature, and 1.1 mL (8.6 mmol) of cyclohexyl isocyanate was added dropwise in 10 min. The mixture solution was stirred for 24 h. The solution was concentrated in vacuo, and then *n*-hexane was added. The resulting precipitates were collected and dried in vacuo to give PFPNCC as a powder. Yield: 0.19 g (96%). ^1H NMR (400 MHz, $CDCl_3$, δ ppm): 7.28–7.92 (m, 6H, fluorene–H), 7.10 (s, 2H, phenylene–H), 4.64 (br, 2H, –NH–), 4.16–4.41 (m, 8H, –CH_2–CH_2–CH_2O–), 3.99–4.09 (m, 4H, –CH_2Br), 3.40–3.55 (m, 2H, –NH–CH–), 2.10– (m, 4H, –CH_2–CH_2OH), 1.83–1.98 (m, 12H, –CH_2–CH_2Br, –CH–CH_2–, fluorene–CH_2–), 1.61–1.71 (m, 8H, –CH_2–), 1.50–1.13 (m, 20H, –CH_2–). The ^1H NMR spectrum of PFPNCC is shown in Fig. S1. ^{13}C NMR could not be measured due to its low solubility. M_n= 1.1×10^4 g/mol, M_w/M_n= 2.0.

3 Results and discussion

The synthetic route of the polymer PFPNCC is summarized in Scheme 1. The precursor PFPOH was synthesized via a Suzuki coupling polymerization [23], and PFPNCC was subsequently obtained by the reaction of PFPOH with cyclohexyl isocyanate. The ^1H NMR spectrum of the product clearly showed a broad carbamate-NH peak at around 3.5 ppm, which supported that the aforementioned reaction was successfully achieved. More details of synthetic methods and assignments of the polymers are summarized in the Experimental section. We also characterized optical properties of PFPNCC. The UV–vis spectrum of PFPNCC showed the maximum absorbance at 370 nm in DMF. The DMF solution of PFPNCC exhibited fluorescence with an emission peak at around 420 nm (λ_{ex} = 370 nm).

First, the fluorescence responsivity of PFPNCC against various heavy-metal ions and transition-metal ones was investigated. Figures 1 and S2 show the quenching behavior of PFPNCC against the addition of various metal ions (Zn^{2+}, Pd^{2+}, Al^{3+}, Pb^{2+}, Ni^{2+}, Mn^{2+}, Li^+, K^+, Hg^{2+}, Fe^{3+}, Cr^{3+}, Co^{2+}, Cd^{2+}, Ca^{2+}, Ba^{2+}, Ag^+ and Cu^{2+}) in DMF. As a result, the addition of metal ions except Cu (II) induced almost no or very weak fluorescence quenching (i.e., less than 10% changes). On the other hand, significant fluorescence quenching by adding Cu(II) was clearly observed. Furthermore, competitive experiments were carried out by monitoring changes in the fluorescence intensity at 420 nm upon addition of the mixture of all tested metal ions to the DMF solution of PFPNCC. No obvious fluorescence quenching was induced by mixed metal ions without Cu(II), whereas a very strong fluorescence quenching by a mixture of metal

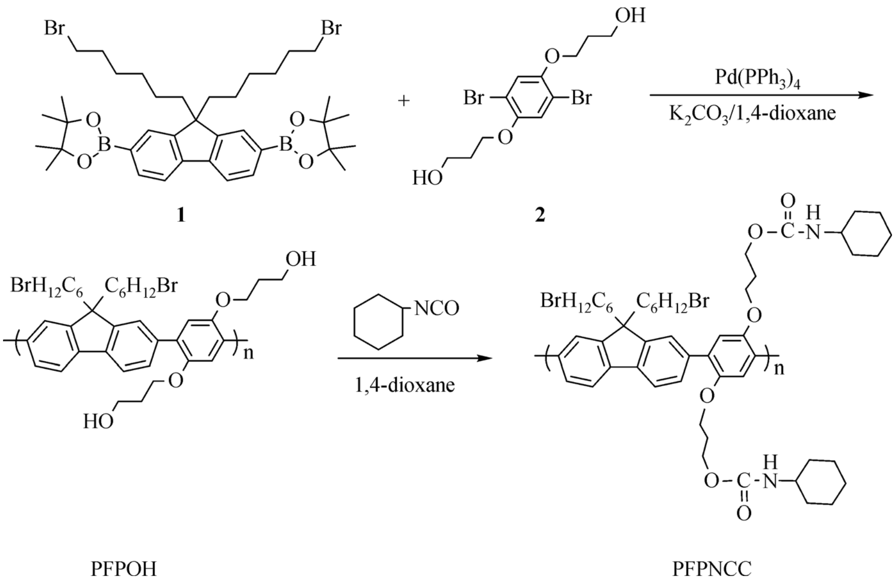

Scheme 1 Synthesis of PFPNCC

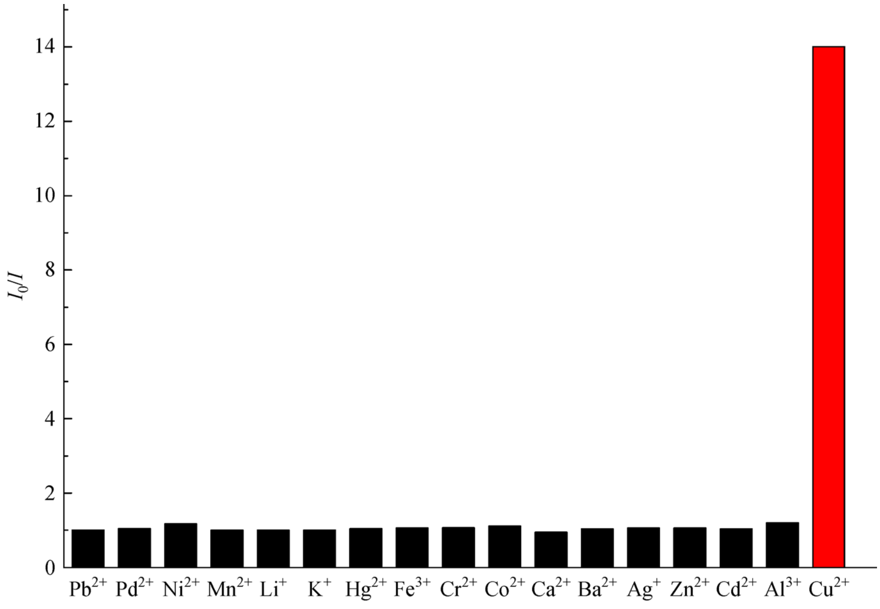

Fig. 1 Fluorescence quenching efficiency of PFPNCC (1.0×10^{-6} mol/L) in DMF by adding metal ions. λ_{ex} = 370 nm, λ_{em}= 420 nm. $C_{\text{Metal ion}}$ = 4 mmol/L

ions with Cu(II) was observed (Fig. S3). Any types of counter anions such as NO_3^-, Cl^-, SO_4^{2-} and ClO_4^- did not affect the fluorescence intensity of PFPNCC. These results demonstrate that the fluorescent chemosensor PFPNCC shows a high selectivity for Cu(II) over other cations.

We further studied the fluorescence response of PFPNCC to an increasing amount of Cu(II) (Fig. 2). As depicted in Fig. 2, a linearly dependent quenching was observed when the Cu(II) concentration was less than 60 μmol/L. The Stern-Volmer quenching constant was estimated to be 1.1×10^4 M^{-1} (Fig. S4). The 3σ detection limit of Cu(II) is ~5 μmol/L, which is lower than the WHO guideline level (30 μmol/L) for copper in drinking water.

To discuss the observed quenching phenomenon, UV–vis spectra was measured for the Cu(II) titration. As shown in Fig. 3, a new weak peak at 435 nm was also observed, which is attributed to a trace of Cu(I) derived from Cu(II) reduction in the presence of PFPNCC with solvent [27]. Upon addition of Cu(II), the color of the solution turned out to be bronze yellow, which could be seen by naked eyes. The similar phenomena and UV–vis spectral changes were also observed in other nucleophilic

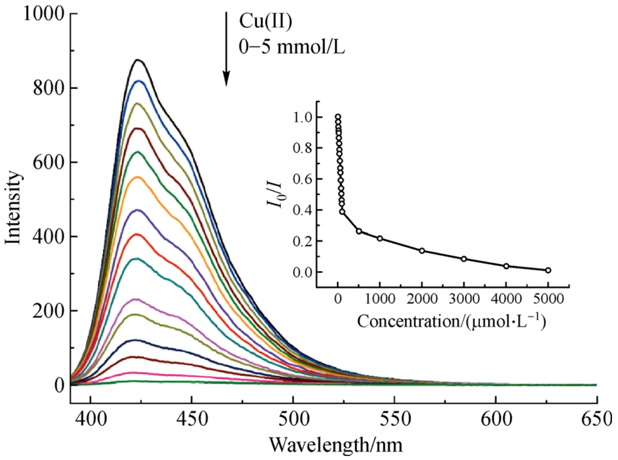

Fig. 2 Fluorescence spectra of PFPNCC (1.0×10^{-6} mol/L) in DMF upon addition of Cu(II). $C_{\mathrm{Cu(II)}}$ = 0–5 mmol/L. λ_{ex} = 370 nm. Inset shows titration isotherm corresponding to the Cu(II)-induced fluorescence quenching

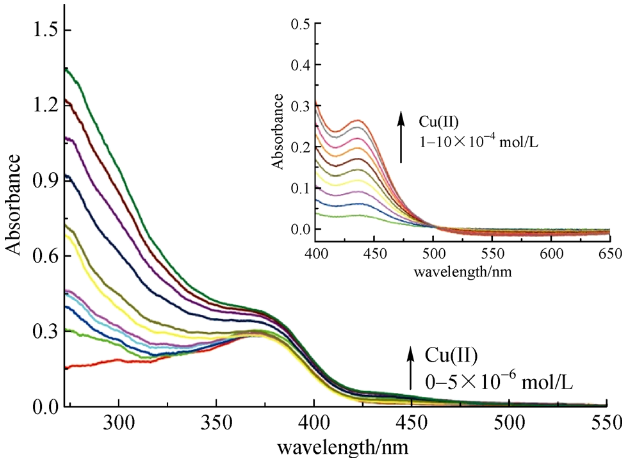

Fig. 3 UV–vis spectra of PFPNCC (1.0×10^{-6} mol/L) in DMF with various concentrations of Cu(II). Inset shows UV–vis spectra of PFPNCC (1.0×10^{-6} mol/L) with higher concentration of Cu (II) in DMF

solvents such as DMSO, but the absorbance peak derived from Cu(I) was not observed in low nucleophilic solvents such as 1,4-dioxane and THF. Figure 4 shows the solvent-dependency of the quenching behavior for the addition of Cu(II). The efficient fluorescence quenching was observed in nucleophilic solvents, whereas weak fluorescence quenching exhibited in low nucleophilic solvents. These results indicate that the fluorescence quenching by Cu(II) is related to the Cu(I) complexes with nucleophilic solvents [25].

The aforementioned UV–vis spectra showed an overlap between the fluorescence spectrum of PFPNCC and the absorbance spectrum of the copper complex. In other words, fluorescence resonance energy transfer (FRET)

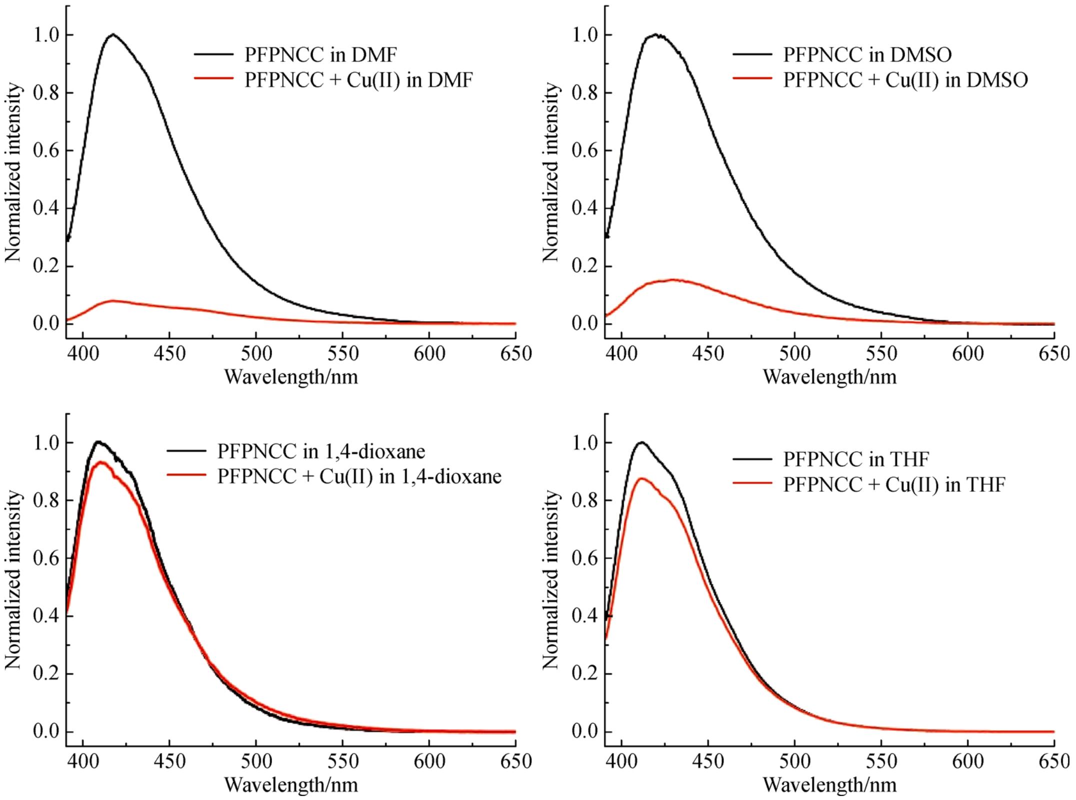

Fig. 4 Fluorescence spectra of PFPNCC in the presence or absence of Cu(II) in various solvents. $C_{\mathrm{Cu(II)}}$ = 4 mmol/L, λ_{ex} = 370 nm

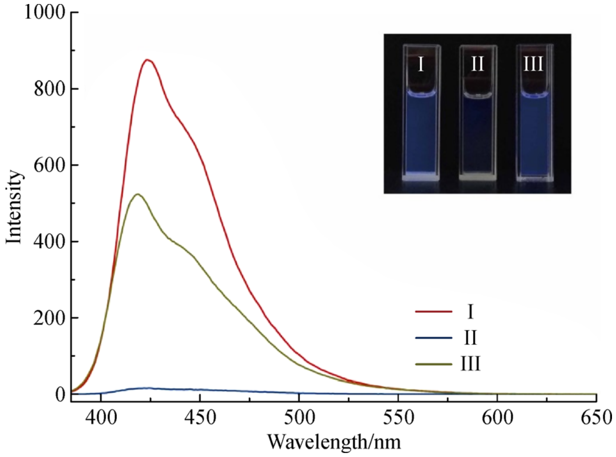

Fig. 5 Fluorescence spectra of PFPNCC (1.0×10^{-6} mol/L) in DMF in the presence or absence of Cu(II) (4 mmol/L) (I: no Cu(II), at 25°C; II: Cu(II), at 25°C; III: Cu(II), at about –75°C). λ_{ex} = 370 nm

and/or photo-induced electron transfer (PET) could be considered for the origin of the quenching phenomenon [28]. The mechanism of FRET depends on an energy transfer without charge separation and reorganization of solvent molecules, and its transfer efficiency is inversely proportional to the sixth power of the distance between a donor and an acceptor. On the other hand, the PET process generates charge separation, and makes an orientation of solvent molecules near by the charged portions. According to those theories, a fluorescence recovery of PFPNCC quenched by the addition of Cu(II) would be observed at low temperature if the fluorescence quenching is induced by PET, because the prevention of the solvent reorganization at low temperature brings about inefficient electron transfer [29]. However, in the case of the FRET process, the fluorescence recovery will not happen [29]. As shown in Fig. 5, the fluorescence intensity of the PFPNCC quenched by the addition of Cu(II) was clearly recovered at low temperature, indicating that the fluorescence quenching at room temperature most probably stems from the PET process followed by the reduction of Cu(II) though the partial fluorescence recovery implies that the FRET process may also exist [29].

To discuss the PET process in detail, the Rehm–Weller equation was employed [30]. The thermodynamic driving force (ΔG_{PET}) should be calculated as:

$$\Delta G_{\text{PET}} = eE°(\text{PFPNCC}^{+}/\text{PFPNCC})$$

$$-eE°(\text{Cu(II)}/\text{Cu(I)}) - W_{\text{p}} - E_{00}(\text{PFPNCC}),$$

where E°(PFPNCC^{+}/PFPNCC), E°(Cu(II)/Cu(I)), W_{p}, E_{00}(PFPNCC) are the oxidation potential of the donor, the reduction potential of the acceptor, the radical ion pair energy and the singlet excitation energy of the donor, respectively. The values of E°(PFPNCC^{+}/PFPNCC) and E_{00}(PFPNCC) are known to be 0.87 V and 3.57 eV, respectively [31]. E°(Cu(II)/Cu(I)) is known to be 0.08 V [32], and the value of W_{p} is negligible [33]. Therefore, ΔG_{PET} = e × 0.87 V – e × 0.08 V – 3.57 eV = – 2.78 eV. As shown the above-calculated value, ΔG_{PET} value is negative from these parameters, suggesting that the PET process can spontaneously occur.

Scheme 2 displays the plausible mechanism of copper ions-induced fluorescence quenching of PFPNCC. First, some Cu(II) ions form complexes with nucleophilic solvents. The electron transfer from the excited state of PFPNCC to Cu(II) ions in the complexes subsequently occurs, resulting in the fluorescence quenching of PFPNCC.

4 Conclusions

In summary, we have developed a highly selective detection method for Cu(II) by using a combination of the “ligand-free” PFPNCC and nucleophilic solvents. The fluorescence of PFPNCC can be efficiently quenched by the addition of Cu(II) in nucleophilic solvents such as DMF and DMSO, but not in low nucleophilic ones such as 1,4-dioxane and THF. This fluorescence quenching may be

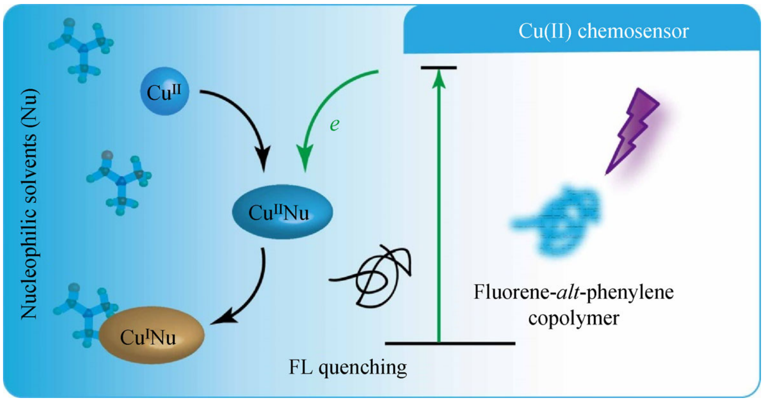

Scheme 2 A plausible mechanism of the fluorescence quenching of PFPNCC by adding Cu(II) in nucleophilic solvents

explained by the PET process in which the Cu(II) ion after forming a complex with nucleophilic solvent is reduced by the excited PFPNCC. Although the recognition of Cu(II) was achieved in organic solvents, the designed chemosensor might be able to detect Cu(II) in biological fluids by incorporating the chemosensor into amphiphilic polymer-gel-matrices [34,35]. Such the "ligand-free" chemosensors would provide a novel strategy for the simpler detection of various metal ions using conjugated polymers in the near future.

Acknowledgements This work was financially supported by the National Basic Research Program of China (Grant No. 2015CB932200), the National Natural Science Foundation of China (Grant Nos. 21604042, 61378081, 21574064, and 21674048), Synergetic Innovation Center for Organic Electronics and Information Displays, Jiangsu National Synergetic Innovation Center for Advanced Materials, the Natural Science Foundation of Jiangsu Province of China (No. BK20150843), NUPTSF (Nos. NY215017, NY211003, and NY215080) and the Innovation Program for Postgraduates Research of Colleges and Universities of Jiangsu Province (No. CXZZ12-0459).

Electronic Supplementary Material Supplementary material is available in the online version of this article at https://doi.org/10.1007/s11705-019-1791-6 and is accessible for authorized users.

References

1. Liu J, Chakraborty S, Hosseinzadeh P, Yu Y, Tian S, Petrik I, Bhag A, Lu Y. Metalloproteins containing cytochrome, iron-sulfur, or copper redox centers. Chemical Reviews, 2014, 114(8): 4366–4469
2. Winkler J R, Gray H B. Electron flow through metalloproteins. Chemical Reviews, 2013, 114(7): 3369–3380
3. Rae T, Schmidt P, Pufahl R, Culotta V, O'halloran T. Undetectable intracellular free copper: The requirement of a copper chaperone for superoxide dismutase. Science, 1999, 284(5415): 805–808
4. Vora S R, Guo Y, Stephens D N, Salih E, Vu E D, Kirsch K H, Sonenshein G E, Trackman P C. Characterization of recombinant lysyl oxidase propeptide. Biochemistry, 2010, 49(13): 2962–2972
5. Kieber-Emmons M T, Qayyum M F, Li Y, Halime Z, Hodgson K O, Hedman B, Karlin K D, Solomon E I. Spectroscopic elucidation of a new heme/copper dioxygen structure type: Implications for O···O bond rupture in cytochrome c oxidase. Angewandte Chemie International Edition, 2012, 51(1): 168–172
6. Multhaup G, Schlicksupp A, Hesse L, Beher D, Ruppert T, Masters C L, Beyreuther K. The amyloid precursor protein of Alzheimer's disease in the reduction of copper(II) to copper(I). Science, 1996, 271(5254): 1406–1409
7. Barnham K J, Bush A I. Metals in Alzheimer's and Parkinson's diseases. Current Opinion in Chemical Biology, 2008, 12(2): 222–228
8. Lee S, Barin G, Ackerman C M, Muchenditsi A, Xu J, Reimer J A, Lutsenko S, Long J R, Chang C J. Copper capture in a thioether-functionalized porous polymer applied to the detection of Wilson's disease. Journal of the American Chemical Society, 2016, 138(24): 7603–7609
9. Tanzi R E, Petrukhin K, Chernov I, Pellequer J L, Wasco W, Ross B, Romano D M, Parano E, Pavone L, Brzustowicz L M, et al. The Wilson disease gene is a copper transporting ATPase with homology to the Menkes disease gene. Nature Genetics, 1993, 5(4): 344–350
10. Shao N, Zhang Y, Cheung S, Yang R, Chan W, Mo T, Li K, Liu F. Copper ion-selective fluorescent sensor based on the inner filter effect using a spiropyran derivative. Analytical Chemistry, 2005, 77 (22): 7294–7303
11. Shen Q, Zhao X, Zhou S, Hou W, Zhu J J. ZnO/CdS hierarchical nanospheres for photoelectrochemical sensing of Cu^{2+}. Journal of Physical Chemistry C, 2011, 115(36): 17958–17964
12. Nuevo Ordóñez Y, Montes-Bayón M, Blanco-González E, Sanz-Medel A. Quantitative analysis and simultaneous activity measurements of Cu, Zn-superoxide dismutase in red blood cells by HPLC-ICPMS. Analytical Chemistry, 2010, 82(6): 2387–2394
13. Yang L, Lian C, Li X, Han Y, Yang L, Cai T, Shao C. Highly selective bifunctional luminescent sensor toward nitrobenzene and Cu^{2+} ion based on microporous metal-organic frameworks: Synthesis, structures, and properties. ACS Applied Materials & Interfaces, 2017, 9(20): 17208–17217
14. Han Y, Ding C, Zhou J, Tian Y. Single probe for imaging and biosensing of pH, Cu^{2+} ions, and pH/Cu^{2+} in live cells with ratiometric fluorescence signals. Analytical Chemistry, 2015, 87 (10): 5333–5339
15. Yun S H, Xia L, Edison T N, Pandurangan M, Kim D H, Kim S H, Lee Y R. Highly selective fluorescence turn-on sensor for Cu^{2+} ions and its application in confocal imaging of living cells. Sensors and Actuators. B, Chemical, 2017, 240: 988–995
16. Hsieh Y C, Chir J L, Wu H H, Guo C Q, Wu A T. Synthesis of a sugar-aza-crown ether-based cavitand as a selective fluorescent chemosensor for Cu^{2+} ion. Tetrahedron Letters, 2010, 51(1): 109–111
17. Kim H N, Guo Z, Zhu W, Yoon J, Tian H. Recent progress on polymer-based fluorescent and colorimetric chemosensors. Chemical Society Reviews, 2011, 40(1): 79–93
18. McQuade D T, Pullen A E, Swager T M. Conjugated polymer-based chemical sensors. Chemical Reviews, 2000, 100(7): 2537–2574
19. Álvarez-Diaz A, Salinas-Castillo A, Camprubí-Robles M, Costa-Fernández J M, Pereiro R, Mallavia R, Sanz-Medel A. Conjugated polymer microspheres for "turn-off"/"turn-on" fluorescence optosensing of inorganic ions in aqueous media. Analytical Chemistry, 2011, 83(7): 2712–2718
20. Dong Y, Koken B, Ma X, Wang L, Cheng Y, Zhu C. Polymer-based fluorescent sensor incorporating 2,2′-bipyridyl and benzo[2,1,3] thiadiazole moieties for Cu^{2+} detection. Inorganic Chemistry Communications, 2011, 14(11): 1719–1722
21. Xing C, Shi Z, Yu M, Wang S. Cationic conjugated polyelectrolyte-based fluorometric detection of copper (II) ions in aqueous solution. Polymer, 2008, 49(11): 2698–2703
22. Jeong Y, Yoon J. Recent progress on fluorescent chemosensors for metal ions. Inorganica Chimica Acta, 2012, 381: 2–14
23. Kaur B, Kaur N, Kumar S. Colorimetric metal ion sensors—a comprehensive review of the years 2011–2016. Coordination Chemistry Reviews, 2018, 358: 13–69
24. Duraisamy U, Naha S, Sivan V. Colorimetric and fluorescent

chemosensors for Cu^{2+}. A comprehensive review from the years 2013–15. Analytical Methods, 2017, 9: 552–578

25. Pu K, Fang Z, Liu B. Effect of charge density on energy-transfer properties of cationic conjugated polymers. Advanced Functional Materials, 2008, 18(8): 1321–1328
26. Sun P, Lin M, Zhao Y, Chen G, Jiang M. Stereoisomerism effect on sugar-lectin binding of self-assembled glyco-nanoparticles of linear and brush copolymers. Colloids and Surfaces. B, Biointerfaces, 2015, 133: 12–18
27. Franc G, Jutand A. On the origin of copper (I) catalysts from copper (II) precursors in C–N and C–O cross-couplings. Dalton Transactions (Cambridge, England), 2010, 39(34): 7873–7875
28. Valeur B, Leray I. Design principles of fluorescent molecular sensors for cation recognition. Coordination Chemistry Reviews, 2000, 205(1): 3–40
29. De Santis G, Fabbrizzi L, Licchelli M, Mangano C, Sacchi D, Sardone N. A fluorescent chemosensor for the copper (II) ion. Inorganica Chimica Acta, 1997, 257(1): 69–76
30. Rehm D, Weller A. Kinetics of fluorescence quenching by electron and H-atom transfer. Israel Journal of Chemistry, 1970, 8(2): 259–271
31. Yang G, Wang W, Wang M, Liu T. Side-chain effect on the structural evolution and properties of poly(9,9-dihexylfluorene-alt-2,5-dialkoxybenzene) copolymers. Journal of Physical Chemistry B, 2007, 111(27): 7747–7755
32. Richardson K A. The manufacture of high temperature superconducting tapes and films. Universal-Publishers, 1999, 4: 26–27
33. Verma M, Chaudhry A F, Fahrni C J. Predicting the photoinduced electron transfer thermodynamics in polyfluorinated 1,3,5-triarylpyrazolines based on multiple linear free energy relationships. Organic & Biomolecular Chemistry, 2009, 7(8): 1536–1546
34. Liu Y, Minami T, Nishiyabu R, Wang Z, Anzenbacher P. Sensing of carboxylate drugs in urine by a supramolecular sensor array. Journal of the American Chemical Society, 2013, 135(20): 7705–7712
35. Minami T, Liu Y, Akdeniz A, Koutnik P, Esipenko N A, Nishiyabu R, Kubo Y, Anzenbacher P. Intramolecular indicator displacement assay for anions: supramolecular sensor for glyphosate. Journal of the American Chemical Society, 2014, 136(32): 11396–11401